HAL open science

Temperature-dependent mechanisms of the atmospheric alteration of a mixed-alkali lime silicate glass

Fanny Alloteau, Odile Majérus, Isabelle Biron, Patrice Lehuédé, Daniel Caurant, Thibault Charpentier, Antoine Seyeux

▶ **To cite this version:**

Fanny Alloteau, Odile Majérus, Isabelle Biron, Patrice Lehuédé, Daniel Caurant, et al.. Temperature-dependent mechanisms of the atmospheric alteration of a mixed-alkali lime silicate glass. Corrosion Science, 2019, 159 (108129), pp.108129. 10.1016/j.corsci.2019.108129 . cea-02265811

HAL Id: cea-02265811

https://cea.hal.science/cea-02265811

Submitted on 20 Dec 2021

HAL is a multi-disciplinary open access archive for the deposit and dissemination of scientific research documents, whether they are published or not. The documents may come from teaching and research institutions in France or abroad, or from public or private research centers.

L'archive ouverte pluridisciplinaire **HAL**, est destinée au dépôt et à la diffusion de documents scientifiques de niveau recherche, publiés ou non, émanant des établissements d'enseignement et de recherche français ou étrangers, des laboratoires publics ou privés.

Distributed under a Creative Commons Attribution - NonCommercial 4.0 International License

Version of Record: https://www.sciencedirect.com/science/article/pii/S0010938X19308388
Manuscript_72f647cb2a5360e1152c313a8a1ec022

Temperature-dependent mechanisms of the atmospheric alteration of a mixed-alkali lime silicate glass

Fanny Alloteau[a,b], Odile Majérus[b], Isabelle Biron[a], Patrice Lehuédé[a], Daniel Caurant[b], Thibault Charpentier[c], Antoine Seyeux[b]

[a] Centre de Recherche et de Restauration des Musées de France (C2RMF), F-75001 Paris, France
[b] PSL University, Chimie Paristech, CNRS, Institut de Recherche de Chimie Paris, F-75005 Paris, France
[c] NIMBE, CEA, CNRS, Université Paris-Saclay, CEA Saclay, F-91191, Gif-sur-Yvette, France

Abstract

The atmospheric alteration of a mixed-alkali lime silicate glass is described as a function of time and temperature. The glass hydration kinetics self-accelerates with time and is considerably enhanced with the temperature. At 80°C, alkali and alkaline earth ions are retained in hydrate-type environments while at 40°C, they are partially leached out forming surface carbonates, in the order Ca^{2+}>Na^{+}>>K^{+}. The temperature dependency of hydrolysis processes, the important role of the hydration energy of cations and the diminished solvation properties of bound water are considered to discuss experimental observations and advance in the understanding of the specificities of glass atmospheric alteration.

1. INTRODUCTION

Glass is a unique material made by melting silica (from sand) with a flux: an alkali and/or alkaline-earth bearing agent that will lower the melt temperature and viscosity. Because of their relatively alkali-rich composition, glasses are more prone to environmental degradation than other oxide-based materials such as traditional ceramics. The degradation always involves the reaction of glass with water, but the physical, chemical and mass transport conditions determine the extent and result of the process. In this paper, atmospheric alteration refers to the degradation of glass by water in the atmosphere (*ie* when relative humidity, RH, is <100%). In the field of Cultural Heritage, this condition excludes, for instance, the water condensation and rain water running off experienced by stained glass windows [1,2] or the saturated environment of buried archaeological objects [3]. Specifically, it is the condition of glasses conserved in atmosphere in the museums, with their diverse nature (glass objects, glazes and enamels). Although this condition is commonly considered as mild, it can give rise to significant damage

© 2019 published by Elsevier. This manuscript is made available under the CC BY NC user license
https://creativecommons.org/licenses/by-nc/4.0/

depending on the glass composition and climatic conditions (temperature, relative humidity, atmospheric pollutants) [4–8] and it is an issue for curators to be able to identify stable from unstable compositions and adjust the environmental parameters to protect the more alterable pieces [5,9–13]. Atmospheric alteration of glass causes short-term issues also in the glass industry, every time that glass is stored in confined in wet conditions (RH > 70%) [14,15]. The consequences of the surface defects induced by the alteration are the reduction of mechanical properties of glass containers or the degradation of the quality of the thin coatings deposited on float glass [16,17]. Recently, glass atmospheric alteration has become an important matter of concern in the assessment of the long-term safety of geological repository of nuclear waste glasses [18–20]. Indeed, it is estimated that the nuclear glass will be exposed to undersaturated conditions for thousands of years [20].

The manifestations of the atmospheric alteration of glass are very specific, and after several centuries of their description, specific and well-defined terms have emerged and been accepted in both the scientific and conservation communities, the most characteristic one being "crizzling" [4]. In particular, Brill [7,10] and Koob [5,11] have identified and accurately described several successive stages of this deterioration that can overlap and be more or less rapid according to both the glass composition and the storage conditions : (i) In an initial stage, alkali salts form on the surface and give to the glass a hazy or cloudy appearance. (ii) In the second stage called incipient crizzling, microcracks of the glass surface appear but they are visible under a microscope only. (iii) In the third stage called full-blown crizzling, the cracking of the glass has grown deeper below the surface and a uniform network of cracks becomes visible to the naked eye. (iv) At the advanced stage of crizzling, flakes fall down from the deeply cracked surface. Eventually, the whole glass piece may desagregate. Note that the appearance of alkali and calcium salts (carbonates or sulfates) forming a hazy veil on the glass surface, is also observed as an initial stage of the atmospheric degradation of industrial soda-lime glasses [14,16,21,22]. Surface cracking is even reported in the most severe conditions (RH = 70% and 80%) [22].

These manifestations correspond to the ambient temperature phenomena ($0 < T < 50°C$). The general mechanisms are relatively well understood [5,21,23,24]: under a wet atmosphere (RH > 60-70%), alkali are leached out of the glass surface and precipitate with acid gases in the adsorbed water film. The alkali-depleted and hydrated leached layer, well observed in numerous studies, has different molar volume and thermal expansion coefficient than the bulk glass, causing its cracking under the effect of cycling temperature and RH, after the layer thickness has reached some threshold. By water diffusion through the leached layer or in the cracks, the alteration progresses and the hydrated layer grows.

Beyond this general picture, numerous questions arise regarding the detailed mechanisms of atmospheric degradation. There is no accurate understanding of the rate-controlling mechanisms, nor of the effect of glass composition and structure. What is exactly the very first step, producing the leached hydrated layer? How does the glass composition influence this step? What is the chemical and structural nature of this alteration layer? What is the rate-controlling mechanism of water diffusion through the layer and how does it depend on composition, RH and temperature? In recent years, the combined effects of RH, environment and glass composition on the very first stage of glass alteration have been studied using SIMS as high resolution chemical imaging and depth profiling technique [23–26]. These studies have highlighted the predominant role of RH in the glass surface alteration and the early mobilization of alkalis towards the surface, with a tremendous effect of the surface composition and structure on the rate of this process.

This study is an attempt to push forward our understanding of the mechanisms of the atmospheric alteration, which occur on a particular glass composition representative of a family of unstable historical glasses [27]. This family is characterized by, approximately, equal weight amounts of Na_2O and K_2O (~10% each), a moderate amount of CaO and MgO (~6%) and of Al_2O_3 (~1%). Deciphering the mechanisms requires to measure the kinetics of the alteration process and study the changes occurring from the macroscopic to the microscopic scale. In an earlier paper [28] we reported the alteration study of this glass at 85 %RH and at 80°C, a high temperature chosen to accelerate the process. Surprising results were found, notably we did not observe the formation of a leached layer associated to alkali salts deposits on the surface. The glass surface hydration was extremely rapid. In the present paper, we describe the atmospheric alteration of the same glass at lower temperature (40°C to 60°C) and 85 %RH. The phenomena on this temperature range were markedly different, and corresponded well to the macroscopic observations reported in the literature, notably the formation of Na- and Ca-rich salts on the glass surface and the crizzling [4,5,23–26]. From the time and temperature dependency of the phenomena, and the precise compositional and structural analysis of the hydrated layers, we propose mechanisms on both temperature ranges and discuss the possible origin of the marked temperature effect.

2. METHODS

2.1. Sample preparation

Experiments were performed on one glass composition: a mixed-alkali lime silicate glass, named glass A ((wt%) SiO_2 71%, Na_2O 11%, K_2O 11%, CaO 5%, MgO 1%, Al_2O_3 1%), representative of several chemically unstable productions of the Middle Ages [27]. This glass was elaborated by

Saint-Gobain Recherche (France) and the composition was checked by Particle Induced X-ray Emission (PIXE). Samples were prepared in the form of plates (1 ×1 ×0.3 cm^3) polished to 1 μm with aqueous suspensions of CeO_2 powders. The polished plates were thoroughly cleaned before the ageing tests, using a 1M sodium dodecyl sulfate (SDS) aqueous solution and ethanol. Time of flight-secondary ion mass spectrometry (Tof-SIMS) analysis conducted on the pristine glass plates after these preparation steps showed an outermost surface layer of about 30 nm significantly depleted in Na, Ca and Mg, and slightly depleted in K (Fig. 3).

For bulk spectroscopy analysis, calibrated glass powders of 32-50 μm, 10-20 μm and 5-10 μm size fractions were also prepared by crushing and sieving the glass. After multiple ultrasonic washing in acetone to remove the fines, their specific surface area σ was measured by the BET method, using a Belsorp Max analyser with krypton as adsorbing gas. The results were σ=1200 ± 100 cm^2/g, 3900 ± 300 cm^2/g and 7800 ± 900 cm^2/g for the powder fractions of 32–50, 10-20 and 5–10 μm respectively.

2.2. Ageing tests

Two different devices were used in parallel to simultaneously control the relative humidity and the temperature of the ageing atmosphere over various time periods: (i) a climatic chamber and (ii) a hermetic box put into an oven and containing a saturated saline solution to control the RH [29]. All details about these devices are given in [28]. The relative humidity was fixed at 85 RH% in all experiments and the temperature was 40°C, 50°C, 60°C or 80°C [28] for various periods of time from 6 h (at 80°C, [28]) to 9 months (at 40°C). With the hermetic box, the 85%RH value was obtained thanks to a solution saturated in KCl. A MadgeTech sensor was inserted in the box to control temperature and RH during the whole experiments. We took care to avoid any liquid water run-off on the samples during the heating and cooling ramps by maintaining the RH below the dew point at every temperature. All tests were performed in static mode (no cycling). In this paper, they are noted V tests or VXh, VXd or VXm tests, where X is the total duration in hours (h), days (d) or months (m) including the ramps. The good correspondence between the two ageing methods (devices (i) or (ii)) has been checked by comparing the alteration phenomena after a 2 months ageing test at 50 °C, 85 RH%, for this glass composition as well as for other compositions. For both ageing methods, the thickness of the alteration layer was the same (10 μm for glass A) and the nature and quantities of surface salts were the same (mainly Ca-bearing carbonates for glass A).

2.3. Characterization methods

The glass surface and sub-surface modifications after a V test were studied at t_1 (end of the V test) and over a 6 months period after t_1, because certain aged glass surfaces continued to transform under the laboratory atmosphere [28]. Sample preparation before the characterization was intentionally very limited. Notably, no rinsing nor polishing were performed, because these operations may be very harmful for the alteration layers integrity [28]. When alteration products were scattered on the surface, we preferred keeping them and taking their presence into account in the interpretation of the characterization data.

Microstructural observation of the glass surface

The surface states of the glass plates were characterized before the V tests (t_o) and several times after the V tests (t_1 and beyond) by optical microscopy in direct or grazing light using a Keyence VHX-5000 numerical microscope with a Z500 objective. This characterization was supplemented by observations with a field-emission gun electronic microscope (FEG SEM) JEOL 7800F, preferentially in secondary electron mode at low acceleration tension (2 to 7 kV), after making the glass surface conductive with a platinum deposit about 1 nm thick. The samples were submitted to a vacuum of about 1 Pa (Pt deposit) and 5.10^{-5} Pa (FEG SEM) during this characterization.

Measurement of the thickness of the alteration layers

Alteration layer thicknesses are noted e_a in this paper. The very small ones (some tens of nm to about 200 nm) were determined from the elementary concentration profiles obtained by Tof-SIMS analysis, with a Tof-SIMS V instrument (Ion-Tof company), using a O_2^+ ion beam (2 keV, about 150 nA) for in-depth abrasion, a Bi^+ ion beam (25 keV, 0.3 pA) for the analysis, and an unfocused electron beam of some eV for the charge neutralization. The crater is 200 µm × 200 µm or 300 µm × 300 µm in size and at its center the analysis zone is 50 µm × 50 µm or 100 µm × 100 µm respectively. The sputtering rate on aged glass plates was determined thanks to mechanical profilometry of the craters (about 0.3 nm/s into the alteration layer for a current of 100 nA). To assess e_a, we considered the distance over which the $^{45}SiOH^+/^{28}Si^+$ ratio is halfway between its near surface concentration (the value measured just after the SiOH surface spike) and its baseline concentration, as a marker of the interface between the alteration layer and the pristine glass, by analogy with a method described in [30] using the $^{1}H^+/^{28}Si^+$ ratio.

For the high enough altered thicknesses (> 200 nm), their evaluation by SEM observations was preferred. When flakes formed on glass plates, their thickness was measured and associated to the alteration layer thickness after we had checked that the flaking indeed occurred near the interface between the alteration layer and the pristine glass. Otherwise, SEM observations were performed on the edge, on a freshly fractured plate, preferentially in backscattered electron mode

172 to visualize the chemical contrast at the interface. These observations were performed in
173 different areas of a same aged glass plate and we report a mean thickness e_a.
174
175 Chemical analysis
176 Elementary compositions of the alteration layers were quantified by Energy Dispersive X-ray
177 spectroscopy (EDX) with the system Bruker QUANTAX 400, at the same time as SEM
178 observations. Analyses were performed either on the surface of the glass plate, outside any defect
179 or crystal, according to the operating conditions and specific quantification method described in
180 [28], or on the edge of the fresh fracture for the alteration layers thick enough. Elementary
181 composition profiles into the alteration layers, from the surface to the alteration layer-pristine
182 glass interface, were obtained by the Tof-SIMS analysis of an area free of salt deposits when
183 possible. Chemical characterization of the alteration products on the surface of glass plates were
184 performed by EDX at low acceleration tension, by X-Ray Diffraction (XRD) with an X'Pert
185 PRO PANalytical instrument using Cu-Kα radiation, and by micro-Raman spectroscopy with a
186 Renishaw Invia instrument using a 532 nm solid-state laser as excitation light.
187
188 Hydration rate measurement
189 The amount of water in the alteration layer, or hydration rate, was measured on glass plates by
190 EDX according to the original method described in [28]. This local measurement corresponds to
191 the water content that has not been evaporated under vacuum, i.e. to the tightly bound water. For
192 a comparison, global weight measurements on glass powders by thermogravimetric analysis
193 (TGA) were performed on a NETZCH STA449 F3 Jupiter equipment, considering that the
194 tightly bound water disappears between about 150 and 500 °C [31].
195
196 Structural studies
197 Structural modifications of the glass at the atomic scale were studied by the mean of solid-state
198 Nuclear Magnetic Resonance (NMR) spectroscopy on pristine and bulk altered glass powder. ^{1}H,
199 ^{23}Na, ^{27}Al and ^{29}Si magic-angle spinning (MAS) NMR spectra were collected on Bruker Advance I
200 and Advance II spectrometers operating at magnetic fields of 7.02 T (300WB) and 11.72 T
201 (500WB), respectively. For these experiments, about 100 mg of a sample was packed in 4 mm
202 outer diameter ZrO_2 rotor and spun from 10 kHz (7.02 T) to 12.5 kHz (11.72 T) using Bruker
203 CPMAS probes. Recycle delay applied for the complete relaxation of nuclear magnetizations was
204 about 1 s for ^{1}H, ^{23}Na and ^{27}Al nuclei and from 20 to 200 s for the ^{29}Si nucleus. ^{1}H spectra were
205 acquired using the Hahn echo pulse sequence (90- T_E-180-T_E-Acq) with a variable rotor-
206 synchronized echo delay T_E. ^{1}H-^{29}Si Cross-Polarization MAS experiments (CPMAS $^{1}H \rightarrow {}^{29}Si$)

were performed with contact times of about 1 ms. Chemical shifts are referenced using a tetrakis(trimethylsilyl)silane sample for ^{1}H (0.2 ppm relative to liquid tetramethylsilane, TMS) and ^{29}Si (for which the highest intensity peak is situated -9.9 ppm from that of liquid TMS), an aqueous solution of NaCl for ^{23}Na (0 ppm) and an aqueous solution of $AlNO_3$ for ^{27}Al (0 ppm). In this paper, we employ the Q^n notation to describe the structure of the silicate network at short distance. Q^n represents a SiO_4 unit with n bridging oxygen atoms (NBO).

3. RESULTS

Contrary to the phenomena at 80°C, temperature at which no carbonate salts formed on the surface of the glass plates during their ageing in the climatic chamber, in the 40-60°C temperature range the formation and growing of the carbonate salts did occur during the ageing. After a time period depending on the temperature, the salts totally covered the surface. Below the crust of salts, a hydrated layer partially depleted in alkali and completely depleted in Ca was observed, characterized by its uniform thickness, its structural homogeneity at the SEM scale, and a flat interface to the pristine glass. When the thickness of the layer reached about 1 μm, the layer cracked and eventually delaminated at some locations. Except an accelerating effect of the temperature, the macroscopic phenomena were similar at 40, 50 and 60°C. The temperature of 40°C was chosen for an in-depth study of the kinetics and chemical and structural characteristics of the alteration. After a short description of the morphological observations at 40, 50 and 60°C, we present the results on the kinetics (as given by the alteration layer thickness as a function of time), and the detailed chemical and structural study of the alteration layer that forms at 40°C, 85 RH%. The results obtained at 80°C, 85 RH% are given for comparison. Note that we name "alteration layer" the entire layer composed of the hydrated layer and the crust of salts on its surface.

3.1. Microstructure of the alteration layers as a function of time and temperature

The SEM images of a selection of altered surfaces are shown in Fig. 1, and the edge of fresh fractures, or of delaminated flakes are shown in Fig. 2. Optical microscopy images, more informative about the optical macroscopic appearance of the samples, as well as complementary SEM images are given in the Data in Brief associated to this paper. The sample aged at 40°C for 12 days provides the earliest stage of alteration in our series of experiments. Two kinds of salts have appeared at this early stage: micrometric salts with sharp angles and faces and submicrometric salts with no specific shape (Fig. 1a). From SEM-EDX and microRaman analysis, the big microscopic salts are assigned to calcite and labelled with number 1 on the

images. The glass surface is still visible below the salts, which appear with a shallow white boundary due to electronic charge effects. At this stage, the alteration layer thickness is less than 100 nm as described later. The coverage of the surface by salts is almost complete after 3 months of ageing. At this ageing duration and beyond, scattered Na enriched carbonates with a characteristic needle-like shape sometimes referred to as "crow's foots"[14] are observed and identified by EDX (Na and C enrichment). These salts are labelled with number 2 in Fig. 1b, c and d. Immediately next to the calcite crystals, other small and shapeless precipitates enriched in Ca, C and O are also observed (Data in Brief Fig. 1d, label 3) and assigned to vaterite. After 9 months of ageing at 40°C, the longest experimental period of the study, the salts form a continuous crust on the top of the glass hydrated layer, which is about 6.5 μm thick (Fig. 2b). The calcite is always recognizable as distinctive crystal stacks with large faces (Fig. 1b, label 1), as are the needle-like Na enriched carbonates (Fig. 1b, label 2). Due to the insufficient amount of salts, only the calcite phase was identified by XRD. The microRaman spectrum of a glass powder (6-10 μm) altered for 6 months at 40°C, bears the distinctive peaks of calcite (283, 715 and 1087 cm^{-1}) and an additional peak at 1071 cm^{-1} that could indicate the presence of pirssonite, a mixed soda-lime carbonate of composition $Na_2Ca(CO_3)_2.2H_2O$ (RRUFF database, reference R040146).
At 40°C, the cracking of the hydrated layer starts after 3 months of ageing, when the hydrated layer is 1±0.2 μm thick. The cracks cut across the salts (see for instance Fig. 1d, the calcite crystal on the left). It means that they have occurred after the formation of the salts, possibly during the ramp to ambient temperature and RH, because of stresses induced by differential dilatation and loss of water. The delamination, which opens an air gap below the flakes, is well put in evidence by the observation of circular interference patterns by optical microscopy (Newton rings) (Data in Brief Fig. 1b). It begins after 6 months of ageing (hydrated layer thickness is 2.5±0.2 μm). Flakes are about 100 μm in length, a size that seems independent of the temperature and time (compare Fig. 1b and d).

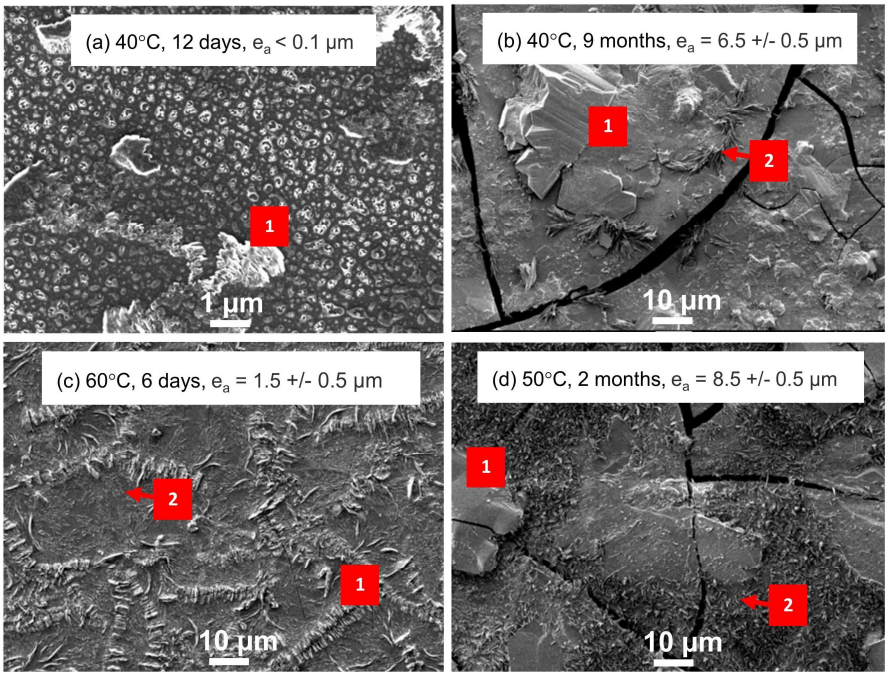

Fig. 1 Surface states of glass A plates immediately after an ageing (t_1 time) at 40 °C (a,b), 60 °C (c) or 50 °C (d), 85 RH%. Secondary electrons SEM images. e_a: alteration layer thickness. Label 1 depicts calcite crystals and label 2 sodium-bearing carbonate crystals.

At 50°C and 60°C, the morphology is comparable but the alteration is more rapid. After 2 months of ageing at 50°C, the alteration layer is composed of an irregular crust of carbonates of thickness up to about 2 µm, and underneath, of a hydrated layer about 8.5 µm thick (Fig. 1d and Fig. 2c). At 60°C and 6 days of ageing, the carbonate salts almost cover the surface, the hydrated layer underneath is already 1.5 µm thick and crossed by cracks (Fig. 1c). Vaterite crystals ($CaCO_3$) were identified (DRX, Raman) together with calcite crystals ($CaCO_3$). The morphology of the calcite crystals is different than at lower temperature: small calcite crystal plates perpendicular to the surface are stacked as chains of several 10 µm length. This microstructure characterized by more numerous and smaller crystals is likely related to a higher nucleating rate of calcite at this temperature. The visual appearance of this sample was completely opaque and white.

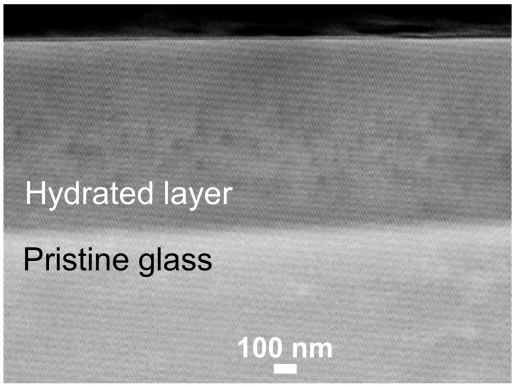

(a) 40°C, 3 months, e_a = 1 +/- 0.2 µm

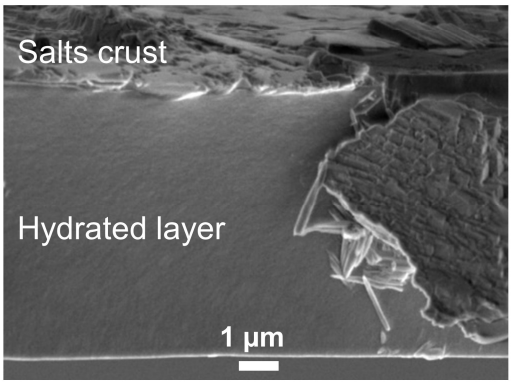

(b) 40°C, 9 months, e_a = 6.5 +/- 0.5 µm

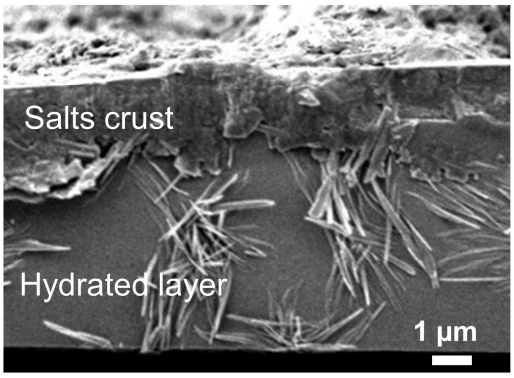

(c) 50°C, 2 months, e_a = 8.5 +/- 0.5 µm

Fig. 2 SEM images of the edge of glass A plates after an ageing at 40 °C (a,b) or 50°C (c), 85 RH%. Secondary electron mode (b, c) or backscattered electron mode (a). e_a: alteration layer thickness.

3.2. Growing kinetics of the alteration layer

As described above, the atmospheric alteration in the 40-60°C temperature range manifests by the concomitant formation of a hydrated layer and of carbonate salts on the top of it. At 80°C, only the formation of the hydration layer is observed during the ageing. Carbonate salts form

after the end of the ageing test, when samples have cooled down to ambient temperature and RH [28]. Interestingly, calcite is never observed on these 80°C aged samples, but only Na carbonates, among which trona only could be identified (a hydroxycarbonate with composition $Na_3(HCO_3)(CO_3).2H_2O$) [28]. Whatever the ageing duration and temperature (40, 50, 60 and 80°C), the hydrated layer has always the same microscopic characteristics: it has a uniform thickness, delimited by a flat and sharp interface with the pristine glass at the SEM scale (about 0.1 μm, Fig. 2a). The dark contrast with the pristine glass is due to partial loss of alkali and lime and hydration (see later), but also probably to a reduced density. The granularity observed at very small scale on the SEM images of the edge is of topological nature (by comparing secondary and back-scattered electrons images). It probably reflects structural inhomogeneity at the nanometer scale. At last, the flatness of the alteration layer-pristine glass interface again demonstrates that the cracking probably occurred during the ramp of temperature and RH at the end of the ageing, otherwise irregularities of the interface around the cracks would be expected.

After the layer has reached one micrometer thickness (1 μm), it cracks and eventually forms delaminated flakes. The concentration profile of the glass beneath the detached flakes was measured by Tof-SIMS for the sample altered at 50°C for 2 months. It is compared with the profile of the pristine, polished glass plates in Fig. 3 (only ionic intensities of $^{39}K^+$, $^{23}Na^+$ and $^{40}Ca^+$ are depicted). The surface of the pristine glass is depleted in Na and K over about 30 nm, due to the polishing by CeO_2 powder in water. The surface of the glass below the detached flakes is less depleted in Na in comparison, and not depleted in K. On the contrary, there is a slight K-enrichment over the first 20 nm below the surface. It means that the delamination occurs within 20 nm of the hydration front. A local K-enrichment around the hydration front has been reported in another study of glass alteration in silica-saturated solution [32]. From this result, it can be considered that the thickness of the flakes corresponds to the thickness of the hydrated layer. The conclusion was the same at 80°C, because the EDX analysis of the glass below the flakes was identical to that of the pristine glass (Table 4 in [28]).

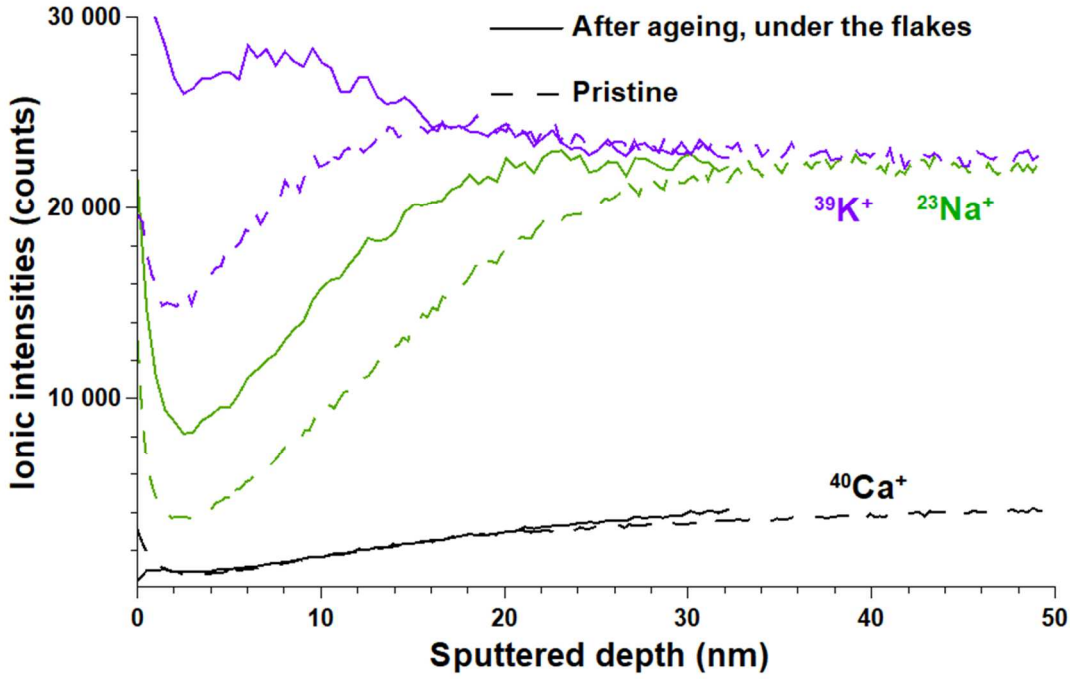

Fig. 3 Ionic intensities in $^{39}K^+$, $^{23}Na^+$ and $^{40}Ca^{2+}$ measured by TOF-SIMS on a pristine glass plate after polishing and washing (dashed curve) and on the glass surface below the flakes of a glass plate aged at 50°C and 85 %RH for 2 months (continuous curve).

The hydrated layer thickness was then measured by Tof-SIMS profiling at short ageing time (6h, 12h at 80°C and 17 days at 40°C), and by SEM at longer ageing time. Values are given in Table 1 and plotted as a function of time in Fig. 4.

In the timescale of the experiments, the growing of the hydration layer tends to accelerate at 80°C and at 40°C. Surprisingly, the hydration kinetics is neither at the square-root of time nor linear, indicating that it is neither simply diffusion controlled nor surface-controlled. Several mechanisms interplay to explain this acceleration that will be discussed later. A complex time dependency has also been found at room temperature for soda-lime silicate glasses, although the very short alteration depths hinders accurate measurement of the kinetics [26].

Moreover, we emphasize that the time and e_a scales are very different in Fig. 4a (80 °C) and Fig. 4b (40 °C). By neglecting the acceleration and assuming a linear rate, the alteration layer thickness increases by approximately 6 µm/day at 80 °C and by about 24 nm/day at 40 °C, which would correspond to a very high apparent activation energy of about 130 kJ/mol. Such a value far exceeds the activation energy reported for silicate network hydrolysis (about 80-85 $kJ.mol^{-1}$ for silicate glasses [33,34]). This result suggests that i) either the rate-controlling mechanisms are different at 80 °C and at 40 °C, or ii) the rate-controlling mechanisms are the same but their

kinetics parameters (activation energy, prefactor) have changed with the temperature.

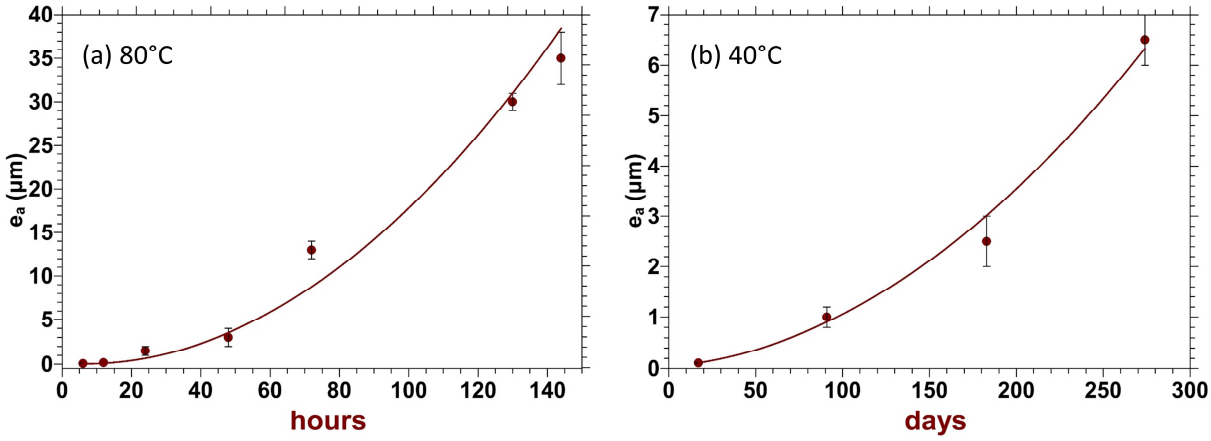

Fig. 4 Alteration layer thicknesses (e_a) of glass A as a function of the ageing duration (numerical values are reported in Table 1). The lines are a guide for the eyes. (a) 80 °C, 85 RH% (climatic oven). (b) 40 °C, 85 RH% (V17d: climatic oven, other ageing durations: hermetic box containing a saline solution of KCl in H_2O).

	80 °C						
	6 h	12 h	24 h	48 h	72 h	130 h	144 h
e_a (µm)	0.055 ± 0.01 *	0.07 ± 0.01 *	1.5 ± 0.5	3 ± 1	13 ± 1	30 ± 3	35 ± 3

	40 °C			
	17 d	3 m	6 m	9 m
e_a (µm)	0.11 ± 0.01 *	1 ± 0.2	2.5 ± 0.2	6.5 ± 0.5

Table 1. Alteration layer thicknesses (e_a) of glass A developed with various ageing durations at 80 °C (climatic oven) or at 40 °C (V17d: climatic oven, other ageing durations: hermetic box containing a saline solution of KCl in H_2O), 85 %RH, as determined by SEM observations or (*) from Tof-SIMS profiles.

3.3. Composition of the alteration layer

The composition of the alteration layer has been measured by EDX with an acceleration tension of 7 kV, on the surface, in an area free of carbonate salts, for the samples aged for 3 months or 6 months at 40°C. At this tension, the analyzed depth is equal to, or less than, 0.6 µm for all the elements of the glass (calculation with the STRATAGem software). Therefore, the alteration layer only contributes to the chemical analysis. The glass plate aged for 9 months at 40°C has developed an alteration layer of 6.5 µm in thickness, which has started to delaminate. It was thus possible to measure the composition on the edge, by scanning a 1 μm^2 area at two distinct

359 locations: near the surface (location 1) and near the interface with the pristine glass (location 2).
360 For the different analyses, the mass elemental fractions totalized 92.5% to 95%. The difference is
361 attributed to the contribution of protons and to porosity (because the contribution of protons is
362 of the order of 1 wt% according to the estimated H_2O content, see below). The elemental
363 fractions reported in Table 2 are normalized to 100% and compared with the composition of the
364 pristine glass A. The elemental ratio Na/Si, K/Si and Ca/Si and the O weight fraction calculated
365 from the cationic composition are also given in Table 2. The difference between the measured O
366 and the calculated O is attributed to water, it allows the calculation of a hydration rate given in
367 the last column. Note that because we used the pristine glass A as a standard for these analyses,
368 the error is minimized and estimated to ~1% for the major elements.
369

	O	Na	Mg	Al	Si	K	Ca	calculated O	Na/Si	K/Si	Ca/Si	H_2O^* wt%
A pristine	59.5	7.58	0.42	0.33	25.2	4.98	1.90	59.5	0.30	0.20	0.075	-
A V3m surface	63.5	5.29	0.58	0.31	25.2	4.95	0.13	56.7	0.21	0.20	0.005	6
A V6m surface	64.4	5.87	0.63	0.29	23.6	5.06	0.11	58.3	0.25	0.21	0.004	9
A V9m edge, 1	64.0	4.72	0.37	0.34	25.6	4.95	0.00	57.0	0.18	0.19	0.00	6.1
A V9m edge, 2	63.73	4.71	0.27	0.42	25.76	5.12	0.00	57.32	0.18	0.20	0.00	5.6

370 **Table 2.** EDX average composition (atom% element with 100% normalization) of the alteration
371 layers of glass A analyzed at the surface or the edge of the glass plates (7 kV acceleration tension)
372 after a V test at 40 °C, 85 RH%, for various ageing duration (hermetic box containing a saline
373 solution of KCl in H_2O). Pristine glass A is used as standard and matrix effects are considered by
374 using the data processing software STRATAGem. * Average hydration rate in weight %
375 estimated from the comparison between the oxygen atomic fraction obtained by EDX and the
376 one calculated by stoichiometry (calculated O column). Concentration ratios R/Si (R=Na, K, Ca)
377 are calculated from EDX results.
378

379 These chemical analyses indicate that the hydrated layer is partially depleted in Na (about 40% of
380 the Na is lost after 9 months), and totally depleted in Ca. It is not depleted in K. Concerning Mg,
381 it is still present in the layer but as a minor element, its analysis is not accurate enough to

comment the variation. Its presence could not be put in evidence in the carbonate precipitates on the surface.

The hydration rate of the layer is 6 to 9 wt%. It can be compared to the hydration rate estimated by thermogravimetric analysis of bulk altered glass powder. According to the thickness of the alteration layer after 6 months of ageing (2.5 μm), the 5-10 μm powder fraction aged for 6 months should be altered in the bulk and this has been verified by ^{27}Al and ^{23}Na MAS NMR. Three thermograms are shown in Fig. 5: the 5-10 μm powder aged for 6 months at 40°C, the 32-50 μm powder aged for 72h at 80°C [28] and a pristine glass A powder. The mass loss below 150-200°C is attributed to weakly bound molecular water, it is around 10 wt% at both 80°C and 40°C (the kink on the 40°C powder thermogram is possibly due to the dehydration of hydroxycarbonates). We observed that the mass loss in this temperature range depends on the conservation conditions of the powders (inside or outside a dessicator for instance), indicating an equilibrium of this weakly bound water with the atmosphere (RH). This water is lost when the samples are put under vacuum in the SEM chamber, so that the mass loss that should be compared with the SEM hydration rate is that measured beyond 150-200°C. On this temperature range, there is a mass loss event between 600 and 700°C in the 40°C altered glass powder, which corresponds to the decomposition of carbonates (CO_2 departure). This event is minimized in the 80°C altered powder because no carbonates formed at this temperature as described before (a few carbonates appeared after the ageing). The hydration rate evaluated by the mass loss in the 150-500°C range, taking into account the contribution of carbonates to the total mass of the 40°C altered powder, is about 8 wt%, in very good agreement with the EDX hydration rate (Table 2). The hydration rate of the 80°C altered powder is similar. The mass of CO_2 in the carbonates is 4.4 wt% of the mass of the 40°C altered powder. It is consistent with the calculated mass of CO_2 in calcite by assuming that all the Ca in this altered glass powder has formed calcite (3.9 wt%), the difference being assigned to the presence of Na-bearing carbonates. This consistency between glass plates data and glass powder data is important to emphasize because it gives robustness to our structural study based on the analysis of altered glass powders.

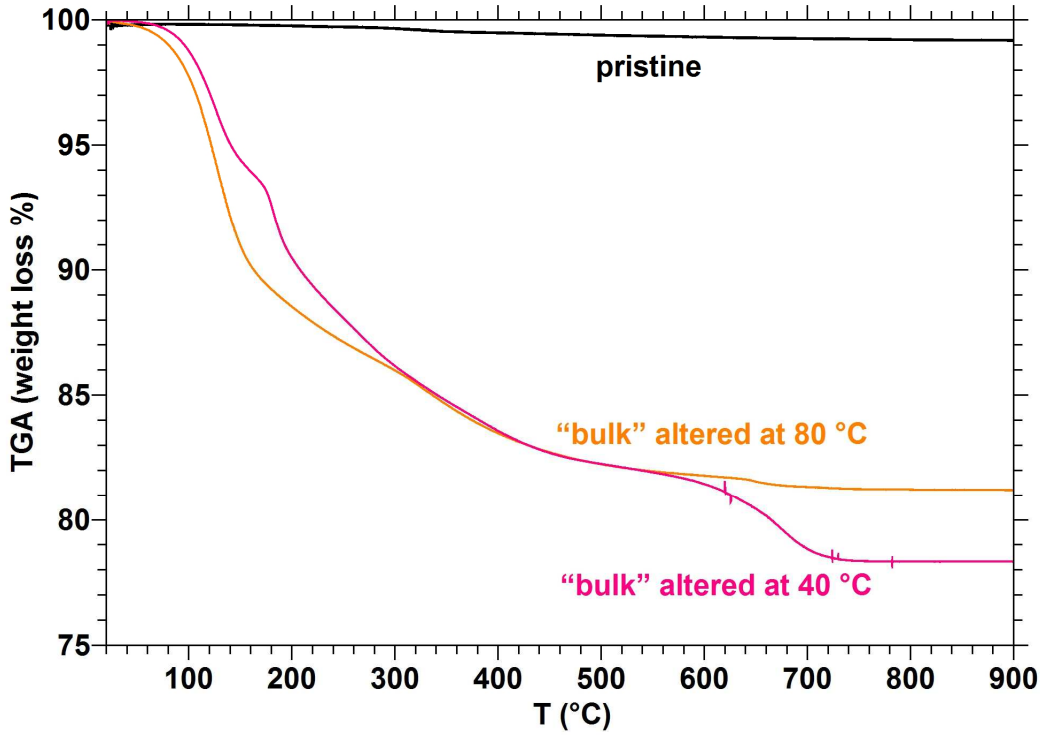

Fig. 5 Thermogravimetric analysis of pristine glass A powder and "bulk" altered glass A powders after an ageing at 80 °C (32-50 µm, V72h, climatic oven) or at 40 °C (5-10 µm, V6m, hermetic box containing a saline solution of KCl in H_2O), 85 %RH. Bulk alteration was checked by ^{27}Al MAS NMR.

By comparing the EDX analysis at the top of the hydrated layer (Table 2, 9 months, location 1) or at the bottom (Table 2, 9 months, location 2), we notice that the hydrated layer is chemically homogeneous. The absence of chemical gradients points out the fact that all the water-glass reactivity occurs at the interface (within 0.1 µm that is our SEM-EDX spatial resolution), leaving behind a hydrated layer that is apparently at equilibrium with the atmosphere and the carbonate salts on the surface. Nevertheless, this equilibrium is only apparent because the Na content of the hydrated layer slowly decreases as a function of the ageing time (compare 3 months and 9 months in Table 2). Another remarkable feature is the complete absence of K depletion, consistent with the absence of K in the carbonate precipitates. There is a striking contrast between the behavior of K (not at all depleted) and Ca (totally depleted).

An attempt to examine the interface between the hydrated layer and the pristine glass has been carried out by TOF-SIMS profile analysis of glass plates aged at 40°C for 17 days and for 3 months. Because of the presence of carbonates on the surface, this attempt was not successful in

accurately profiling the interface, but it confirmed the extent of the depletion of the various cationic elements. The description of this result is placed in the Data in Brief associated to this paper.

3.4. **Atomic structure of the alteration layer**

Glass powders of 5-10 μm, 10-20 μm and 32-50 μm have been aged for 6 months at 40°C, or 2 months at 50°C, or 12 days at 60°C (85 %RH) respectively, in order to produce alteration in the bulk. The spectra of the bulk altered glass powder (32-50 μm) aged at 80°C published in [28] are reported also for comparison. The ^{1}H MAS NMR spectra at the different temperatures are compared in Fig. 6a while the Hahn echo (HE) acquisitions of the 40°C altered powder are shown as a function of varying echo time T_E in Fig. 6b (peaks of the species experiencing the strongest homonuclear ^{1}H-^{1}H dipolar interactions – thus in a dense proton network – decrease faster; thus using a variable echo delay helps identify different environments). These series of HE spectra put in evidence at least 5 hydrated species in the aged glass: a broad signal at about +5 ppm, two high frequency signals at +10 ppm and +14 ppm and two weak, narrow signals at about 0-+3 ppm. The broad signal centered at +5 ppm dominates in the spinning sidebands manifold, and its relative intensity decreases rapidly with increasing T_E. Following the literature [35,36], this behavior allows to assign it to molecular water, because the strong homonuclear dipolar coupling in H_2O associated to its high concentration induce shorter spin-spin relaxation time (T_2) and irreversible loss of this signal in the central band of the HE spectra at high echo time, with respect to the other hydrated species with weaker homonuclear dipolar coupling. Moreover, the relative intensity of this signal decreases faster in the spinning sidebands than in the central band (this is particularly visible in the T_E=120 μs spectrum in Fig. 6b). It means that molecular water does not account for all the intensity at about 5 ppm. Note that because of these irreversible losses that depend on the hydrated species (different T_2 values), it is not really possible to quantify the proportion of these species by simulating the central band intensity. Besides, the widths of these spectra have two main origins: i) the distribution of isotropic chemical shifts (inhomogeneous width) and ii) the residual homogeneous width due to the incomplete averaging (i.e., cancellation) of the dipolar couplings by the MAS. It is highly probable that in our glasses, using a MAS spinning frequency of 10 kHz, the inhomogeneous width dominates, as it has been demonstrated in hydrous aluminosilicate glasses [37].

By increasing the echo time, the water signal is filtered and the other contributions with longer T_2 appear. The two peaks at +10 ppm and +14 ppm most likely belong to the same broad and asymmetrical distribution of intensity between +14 and +3 ppm, with most of the intensity on

the intermediate to high frequency side. This broad component corresponds to OH groups with a distribution of hydrogen bonding strength. Indeed, a correlation between the chemical shift and the O-H…O distance, which measures the strength of the hydrogen bonding, has been reported for long in the literature and supported by theoretical calculations [35,37]. The O-H…O distances that give account of the +10 and +14 ppm chemical shifts are 2.65 Å and 2.50 Å respectively. Such high ^{1}H isotropic chemical shifts revealing very strong hydrogen bonding of the OH groups are commonly observed in alkali silicate crystal hydrates [35,38,39] and in hydrous alkali silicate glasses [40–42]. They are not observed in hydrous silica [43], nor in glasses altered by immersion in liquid water, which are depleted in alkalis and of which ^{1}H isotropic chemical shifts do not exceed 8 ppm [44]. Therefore, they are related to the presence of alkalis and non-bridging oxygens (NBO) and indicate hydrogen bonding between a Si-OH group and a Si-O$^-$(M$^+$) group possibly connected to the same Si [38,45] with M$^+$ being an alkali, as in the following picture where (a) is an intratetrahedral H-bonding in a hydrated Q^2 species, (b) is a H-bonding between neighboring tetrahedra and (c) is a H-bonding between adjacent, but not neighboring tetrahedra:

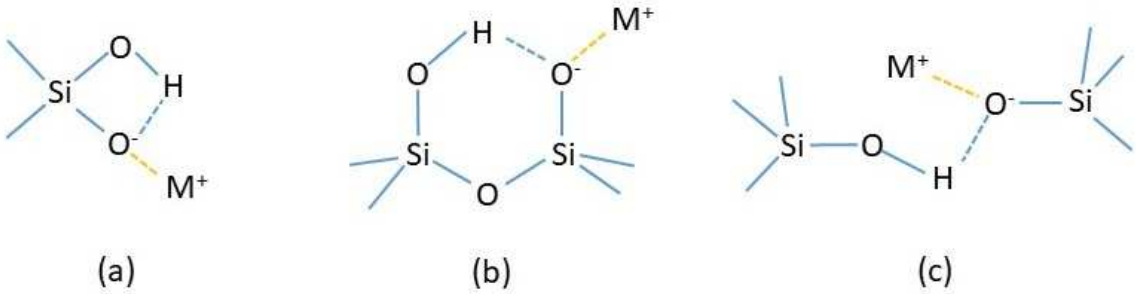

In the cases (b) and (c), the two tetrahedra are noted Q^3-H and Q^3-M,H to refer to the H-bond of this species. The O(H)-O- distance is expected to be about 2.64 Å in the intratetrahedral H-bonding (a), between 2.55 Å and 2.75 Å in H-bonding between neighboring tetrahedra depending on the nature of the alkali, in the order K<Na<Li (b) [40], and distributed in (c). Note that in these structural arrangements, the protons are almost structurally equivalent to modifier cations. Such a proton species exists in $KHSi_2O_5$ crystal structure (with δ_{iso}= 15.6 ppm) and it has been proposed that similar $NaHSi_2O_5$ units exist in sodium silicate crystal hydrates like sodium disilicate hydrates (^{1}H δ_{iso}= 15.3 and 18.7 ppm, [38]) and hydrates with high silica content (octosilicate, ^{1}H δ_{iso} = 16 ppm, magadiite, ^{1}H δ_{iso}= 14.9 ppm and kenyaite, ^{1}H δ_{iso} = 15 ppm, [40]) with the difference that Na$^+$ ions are also surrounded by water molecules. In these hydrates, by examining the ^{1}H NMR line widths and the ^{2}H (D) quadrupolar parameters of OD groups in deuterated samples, the protons of the H-bonded OH may be considered as rigid with respect to the NMR time scale, and they do not exchange with protons of water molecules

[39,45].

At last, narrow, weak signals at low chemical shift (0-+3 ppm) are assigned to isolated OH groups, because of their weak H-H dipolar coupling and low chemical shift. These species may be isolated Si-OH or M-OH groups, possibly in crystalline environments [35,40].

The comparison of the MAS spectra in Fig. 6a indicates that the relative proportion of molecular water and OH groups vary with the temperature of ageing in a regular way, with more molecular water at high temperature. The total amount of water (H_2O+OH) has not been measured in these powders at the time of the NMR experiment, so that it is difficult to draw any conclusion from this tendency. As we have noticed with the TGA measurements, there is an equilibrium between the weakly bound molecular water in the layer and the atmospheric humidity. All the spectra have been measured in the same atmosphere. Either the alteration layer produced at high temperature (60°C, 80°C) takes more molecular water, or the relative proportion of the species differ: the answer needs a careful study with control of the total H_2O content.

The HE acquisitions (T_E = 320 µs) of the glass powders aged at the different temperatures are given in Fig. 6c, to compare the spectra after filtering the water (and Si-OH species close to this water having the shortest T_2). These spectra are very similar regarding the number, positions and relative intensities of the peaks. This points out a structural similarity of the hydrated layer produced in the 40°C-80°C temperature range. The quantitative analysis of the Si-OH and water speciation would require a deeper experimental study.

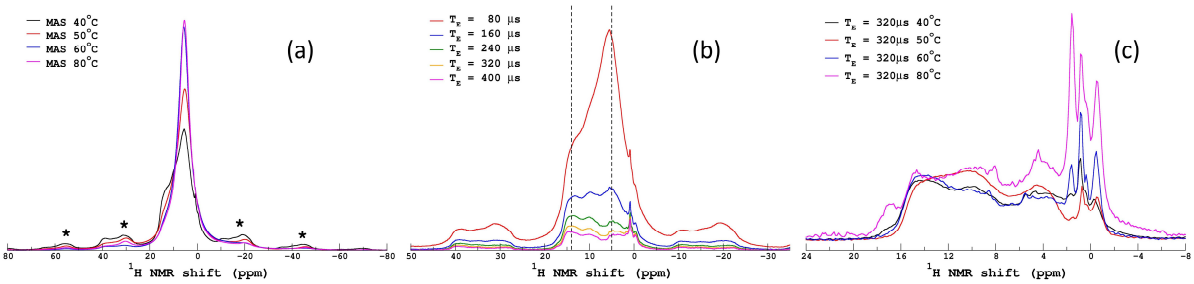

Fig. 6 (a) ^{1}H MAS NMR spectra of bulk altered glass A powders after an ageing at 40°C, 50°C, 60°C, 80°C and 85 %RH. The spectra are normalized to the same area including the spinning side bands. *: spinnnig sidebands. (b) Hahn echo acquisitions with variable echo delays T_E of the bulk altered powder produced at 40°C, 85 RH%. (c) Hahn echo acquisitions (T_E = 320 µs) of the bulk altered glass A powders produced at the different temperatures. The spectra are normalized in height to the peak intensity centered around +14 ppm.

The ^{29}Si MAS NMR spectra of the pristine and altered glass A at 40°C and 80°C are depicted in Fig. 7a. Intermediate temperatures give similar spectra and are therefore not shown. The

simulation of the pristine glass spectrum gives 35% of Q^4 species at -103 ppm and 65% of Q^3 species at -92 ppm, in excellent agreement with the glass A composition assuming homogeneous distribution of the NBOs in the silicate network, and with the chemical shifts in the literature [46]. After ageing in humid atmosphere at both temperatures, the Q^4 band decreases very significantly while the Q^3 band maintains its intensity and is enlarged on the high frequency-side. The apparition of a few Q^2 units might explain part of this enlargement, but the main part is probably owed to the widening of the Q^3 chemical shift distribution because of a greater variety of Q^3 species (Q^3-H and Q^3-Na and all the intermediate Q^3-H,Na species with varying H-bonding strength). We notice that there is a double-peak in the Q^3 component of the glass powder aged at 80°C, which is not visible in the powder aged at 40°C. This double-peak appears in the $^1H \rightarrow {}^{29}Si$ CP MAS spectrum of this latter powder, with a long contact time (2 ms, Fig. 7b). Indeed, although no efficient $^1H \rightarrow {}^{29}Si$ cross-polarization could be achieved on the 80°C altered powder (possibly because of a high amount of short T_2 H species), it was possible to acquire $^1H \rightarrow {}^{29}Si$ CP MAS and HETCOR spectra on the 40°C altered powder, shown in Fig. 7b and 7c. At short contact time (0.5 ms), all the hydrated species are in the vicinity of a wide distribution of Q^3 (and possibly Q^2) units. However, at long contact time (2 ms), two additional Q^n species show up at a longer distance to protons: a Q^4 signal at about -109 ppm, remarkably narrow, and a Q^3 signal at about -96 ppm analogous to the low-frequency peak in the 80°C altered powder. Thus, we propose to assign the Q^3 low-frequency peak (-96 ppm) to Q^3-Na species, or to Q^3-Na,H species undergoing weak H-bonding (long O---H distance), and the high-frequency peak (-88 ppm) to Q^3-H species, or to Q^3-Na,H species undergoing strong H-bonding (short O---H distance). This assignment is consistent with the fact that Q^3-Na species are expected to be more abundant in the 80°C altered glass, because it has retained all the alkali [28] with respect to the 40°C altered glass that has lost up to 40% of the alkalis. On the other hand, the narrow Q^4 signal is not expected in a glass. Its ^{29}Si chemical shift is the same as in cristobalite [47]. This suggests the possible presence of locally ordered re-polymerized areas in the hydrated glass at 40°C, in agreement with hints of a re-polymerized component in the corresponding Raman spectra (see below).

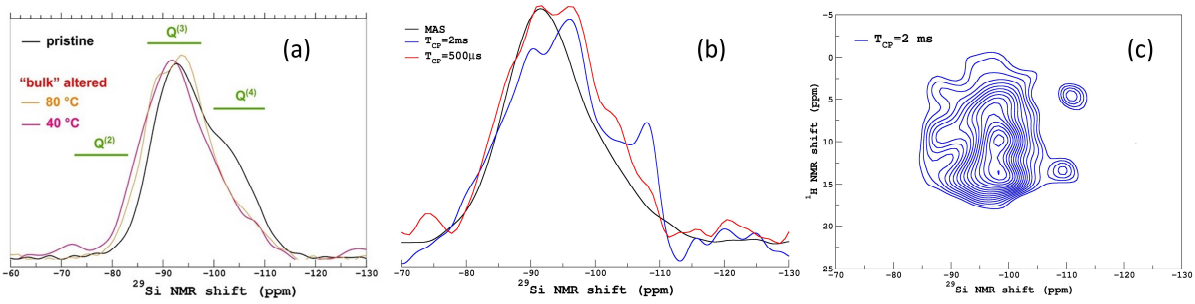

Fig. 7 (a) ^{29}Si MAS NMR spectra of bulk altered glass A powders after an ageing at 40°C or 80 °C, 85 %RH. The ^{29}Si NMR MAS spectrum of pristine glass A powder is reported for reference. (b) CPMAS ^{1}H-^{29}Si acquisition for two contact times (T_{CP}) of the bulk altered glass A powder aged at 40°C, 85 RH% and (c) HETCOR ^{1}H-^{29}Si acquisition of the same powder for T_{CP}=2 ms.

This NMR study has been completed by ^{23}Na MAS NMR and ^{1}H → ^{23}Na CP experiments on the altered powders, reported in Fig. 8. The ^{23}Na MAS NMR spectrum of the pristine glass A shows a broad asymmetrical profile which is typical of Na in alkali silicate glasses [48,49]. The broadening originates from the distribution of both the isotropic chemical shift and the second-order quadrupolar interaction. These spectra have been fitted following the procedure described in [50]. The fit of the 40°C altered powder is shown in Fig. 8b and the fit parameters are reported in Table 3.

Comparing the pristine glass A and the glass powder aged at 80°C, the ^{23}Na NMR parameters indicate a very slight increase of the Na-O mean distance, and an environment that has become more centrosymmetrical with the alteration (see discussion in [28]). The ^{23}Na NMR spectrum of the glass powder aged at 40°C bears two signals, the signal of Na^+ in the hydrated glass, having a ^{23}Na δ_{iso}~ -2.7 (2.3) ppm and C_Q ~1.1 (0.5) MHz (standard deviation under brackets) and the sharp signal of Na^+ in a crystalline phase that may possibly be assigned to Na, Ca mixed hydrated carbonates such as gaylussite ($Na_2Ca(CO_3)_2.5H_2O$) that has been identified on the Raman spectrum (Fig. 9) although no ^{23}Na NMR reference spectrum could be found to confirm. The ^{1}H → ^{23}Na CPMAS NMR spectrum does not exactly overlap the MAS spectrum (Fig. 8a). This indicates a complex distribution of environments for Na in this powder aged at 40°C, with, in average, a more centrosymmetric character (lower mean C_Q) and larger Na-O distances (lower mean δ_{iso}) than in the powder aged at 80°C. The ^{1}H → ^{23}Na correlated component and the 80°C altered glass have very similar ^{23}Na parameters although (Table 3).

In the ^{1}H → ^{23}Na HETCOR spectrum in Fig. 8c, the sharp signal is correlated with protons at low-frequency only, while the signal of Na^+ in the hydrated glass is correlated with all the proton frequencies, in particular that around +14 ppm consistently with their attribution to OH groups

forming hydrogen bonds with NBOs. Thus, Na^+ ions are in close vicinity of all the hydrated species (OH and molecular H_2O) in the glass hydrated at 40°C as well as in the glass hydrated at 80°C [28]. However, at 40°C, part of the Na^+ ions have migrated and formed carbonates.

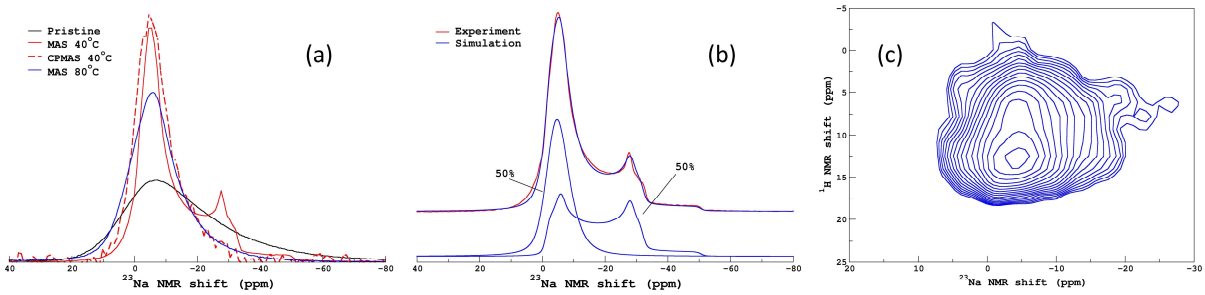

Fig. 8 (a) ^{23}Na MAS NMR spectra of pristine and bulk altered glass A powder after an ageing at 80 °C, 85 %RH (32-50 µm, V72h, climatic oven) or at 40 °C, 85 %RH (5-10 µm, V6m, hermetic box containing a saline solution of KCl in H_2O). Spectra are normalized to the same area. (b) Fit and decomposition of the spectrum of the 40°C altered powder. (c) HETCOR $^1H \rightarrow {}^{23}Na$ acquisition with a contact time of 0.8 ms of the 40°C altered powder.

	^{23}Na δ_{iso}	C_Q (MHz)	η_Q	Assignment and proportion
Pristine glass A	+3 (9)	4.3 (1.4)	0.6	
Bulk altered glass 80°C	-1 (4)	1.6 (0.7)	0.6	
Bulk altered glass 40°C MAS	-2.7 (2.3)	1.1 (0.5)	0.6	Large component 50%
	4.8	3.9	0.15	Crystallized component 50%
Bulk altered glass 40°C CP MAS $^1H \rightarrow {}^{23}Na$	-1 (3)	1.8 (0.4)	0.6	

Table 3. ^{23}Na NMR fit parameters of the bulk altered glass A powder aged at 40°C. The parameters of the pristine glass and 80°C altered powder are also given for comparison.

The Raman spectra of the pristine and bulk altered glass powders are compared in Fig. 9. The Raman spectrum of the pristine glass A is typical of alkali silicate glasses with O/Si ratio between 2.25 (tetrasilicate composition) and 2.5 (disilicate composition), of which silicate network is mainly composed of Q^4 and Q^3 units. In the high-frequency range, the band at 1100 cm^{-1} is assigned to the stretching modes of Q^3 units while the small band at 950 cm^{-1} is related to Q^2 units [51,52] likely bound to Ca^{2+} and Mg^{2+} cations [53]. In the intermediate frequency range (300-700 cm^{-1}), the Raman intensity stems from the Si-O-Si bending modes of the silicate

network, and directly reflects the Si-O-Si angle distribution. In alkali silicate glasses, this distribution is bimodal, with high and widely distributed Si-O-Si angles in polymerized silica-type regions, and weaker, less distributed Si-O-Si angles in depolymerized sodo-silicate type regions. The first population is responsible of the broad low-intensity signal around 460 cm^{-1}, while the second population gives rise to the peak at 545 cm^{-1} [54]. The Raman spectra of the bulk altered glass powders are severely modified. The Q^n stretching band downshifts to 1030 cm^{-1} for the two ageing temperatures 40°C and 80°C. The interpretation of the Raman intensity in the 1020-1040 cm^{-1} range is controversial. Zotov and Keppler assign it to Q^3 species distinct from those causing the 1100 cm^{-1} band [55]. Because intensity in this region is present in alkali tectosilicate glasses [56] and following theoretical results [57], Le Losq et al. ascribe it to asymmetrical stretching of polymerized units [58]. Considering the NMR results described above on these altered powders, we prefer the interpretation of Zotov and Kepler and propose to assign this band to Q^3 units with strong hydrogen bonding of their NBO (these units will be noted Q^3(Na,H) in this paper). It is expected that this hydrogen bonding induces a low frequency shift of the Q^3 stretching band, by weakening the Si-NBO bond. Beside, the well-defined Q^2 peak at 950 cm^{-1} interestingly disappears, and a weak intensity signal around 910 cm^{-1} appears that has been clearly identified as the stretching mode of Si-OH bonds [55,57]. The decrease of the 800 cm^{-1} band, ascribed to the "cage-like" motion of Si in the Q^4 tetrahedron has been observed by Zotov and related to the depolymerization of the network. The intermediate frequency range shows more variations according to the ageing temperature. At 80°C, the Si-O-Si bending band at 545 cm^{-1} is still present with a decreased intensity, and a new narrow band at 665 cm^{-1} has appeared. The spectrum of the 80°C altered powder is very close to the spectra of Cultural Heritage glass replica aged at 60°C in humid atmosphere with 100 % RH published by Robinet et al. [59]. The narrow band at 665-670 cm^{-1} has been proposed as a characteristic feature of these alteration conditions. It is assigned to Si-O-Si symmetrical bending in depolymerized and isolated components of the network, such as Q^2 chains in pyroxenes (of which Si-O-Si bending frequencies are in the range 650-700 cm^{-1}) [60]. Actually, it strongly evokes the intense and characteristic band at 668-672 cm^{-1} in calcium silicate hydrate (C-S-H), which consists in Q^2 chains and Q^1 dimers [61]. This assignment is consistent with the retention of Ca^{2+} ions in the hydrated layer at 80°C. In the spectra of the powder aged at 40°C, this peak is absent, and the intensity of the broad band with maximum at 460 cm^{-1} has markedly increased, which can be related to partial re-polymerization of the network. Moreover, the Si-O-Si bending peak originating from the depolymerized component of the network has shifted to lower frequency, from 545 cm^{-1} (characteristic of the NS3 composition [54]) to 520 cm^{-1} (between NS4 and NS7 composition). This downshift

632 indicates a lower content of alkalis in the altered glass, consistently with the chemical analysis of
633 the alteration layer that shows a loss of up to 40% of the Na^+ ions. On the other hand, the sharp
634 peaks in the spectra of the 40°C altered powder correspond to carbonates, among them calcite
635 (peaks at 282, 712 and 1086 cm^{-1}), gaylussite ($Na_2Ca(CO_3)_2.5H_2O$, peaks at 260 and 1071 cm^{-1}),
636 the peak at 218 cm^{-1} remaining unidentified.

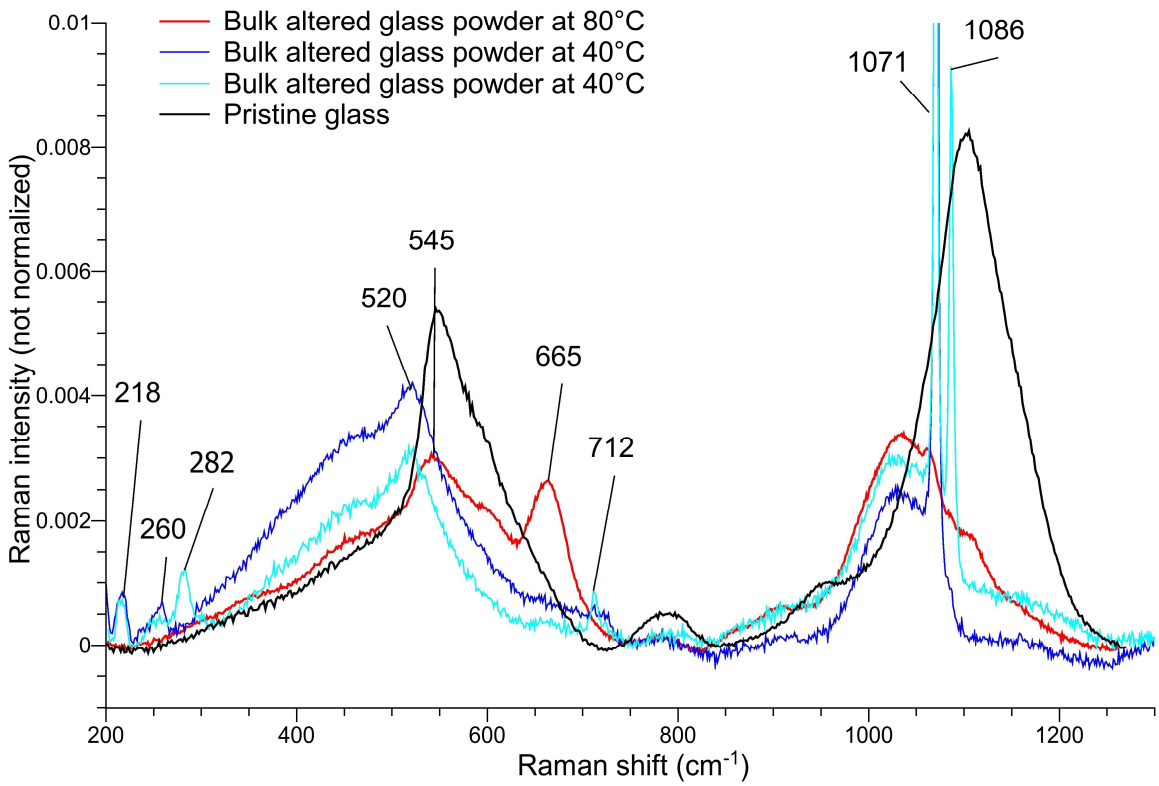

637

638 **Fig. 9** Raman spectra of the pristine glass A (black curve) and of bulk altered glass A powder
639 after an ageing at 80 °C, 85 %RH (32-50 µm, V72h, climatic oven) (red curve) or at 40 °C, 85
640 %RH (5-10 µm, V6m, hermetic box containing a saline solution of KCl in H_2O). Because of the
641 presence of carbonates in the powder aged at 40°C, there is a variability in the Raman spectra, so
642 that two spectra are shown for this powder (blue and cyan curves).

643

644 **4. DISCUSSION**

645 The alteration layer produced in glass A in atmospheric conditions (85 %RH) is composed of a
646 hydrated layer with no depletion of any chemical element at 80°C, and of a hydrated layer
647 depleted in Ca (totally) and Na (partially) with carbonate salts on the surface at 40°C. The
648 concentration of tightly bound water is about 5 to 10 wt% with no clear indication of a different
649 water content at 80°C and at 40°C. This water is present as molecular H_2O and as Si-OH species
650 with a wide distribution of H-bonding strengths, the strongest ones connecting H to NBO's like
651 in alkali silicate hydrates. From ^{29}Si NMR and Raman spectra, the silicate network has

depolymerized with the ageing and bears primarily Q^3-H (Si-OH) and Q^3-M,H (Si-OM---H with M = Na or K) units, although at 40°C a part of the network has also re-polymerized, possibly after the departure of some Na^+ and Ca^{2+} ions. We emphasize that the structure of the hydrated layer produced in these atmospheric conditions markedly differs from the structure of the alteration layer, often called « alteration gel », produced in immersion conditions. In the latter conditions, the gel is completely depleted in alkalis and the silicate network has re-polymerized, following either *in situ* condensation reactions or silica precipitation from the solution [62]. In atmospheric conditions, the hydrated glass still contains a significant amount of alkalis and NBO's, and is closer to an alkali silicate hydrate than to an alteration gel. As in hydrates, the dense network of hydrogen bonds probably contributes to the stability of the layer [63].

In the hydrated layer, Na^+ ions are surrounded by NBO's, OH groups and molecular water as inferred from the $^1H \rightarrow {}^{23}Na$ CP NMR spectra. They are thus totally or partially solvated explaining that they are finally detached from the NBO's and leached out of the glass. There is no structural information on the environment of K^+ and Ca^{2+}, but because leaching of K^+ is never observed in these experiments, we may propose that K^+ ions are still primarily bound to NBO's in the hydrated glass. On the contrary, at 40°C, Ca^{2+} ions are primarily solvated because they are totally leached out, forming carbonates on the glass surface. These observations can be summarized by considering the following equilibrium in the hydrated glass:

$$\text{Si-OM} + H_2O \leftrightarrow \text{Si-OH} + MOH_{aq} \quad (1)$$

Where M are alkali (Na^+ or K^+) or half a Ca^{2+} ion and *aq* refers to the hydrated state of MOH. This well-known equilibrium has been referred to as « ion exchange » [64] but it is more exactly an acid-base reaction of water with the NBO sites, implying diffusion of molecular water and its immobilization by the formation of silanol groups [65,66]. It can also be viewed as a complexation equilibrium of the M cations with the silicate polyanionic network, associated to the acid-base reaction ((1) = (2)+(3)) :

$$\text{Si-OM} \leftrightarrow \text{Si-O}^- + M^+aq \quad (2)$$

$$\text{Si-O}^- + H_2O \leftrightarrow \text{SiOH} + OH^-aq \quad (3)$$

Reaction (2) points out the fact that there is a balance between the solvation (or hydration) of the M^+ cations and their inner sphere complexation on the silicate NBO sites. A similar balance governs the selectivity of clays for alkali ions and results in the order $Cs^+ > K^+ > Na^+ > Li^+$, because the energy of hydration that goes in the reverse order overrides the energy of complexation in the interlayer (Teppen and Miller, 2006; Rotenberg et al., 2009). Similar ionic selectivity has been found in the alteration gels of the International Simple Glass (ISG) formed in Si-saturated solutions with increasing alkali salts concentrations : the K^+ or Cs^+ ions provided by

686 the solution almost totally substitute the Ca^{2+} ions in the gels, while Na^+ and Li^+ ions do not [69].
687 The authors interpreted these results by analogy with the selectivity in clays, suggesting that it is
688 mainly determined by the affinity of cations for hydration, rather than for pore surface
689 complexation: K^+ and Cs^+ are "hydrophobic" cations that prefer complexation. We propose to
690 use the same analogy to explain our observation that cationic species are detached of the NBO's
691 in the order $Na^+>K^+$. Na^+ ions are more stabilized by solvation than K^+ and are thus more
692 quantitatively converted to solvated species, able to migrate under a chemical potential gradient.
693 Moreover, in alkali disilicate hydrates, K^+ are not coordinated to molecular H_2O and form
694 "$KHSi_2O_5$" units, while Na^+ are coordinated to NBO *and* H_2O [39]. It is then possible that Si-
695 OK units are particularly stabilized in the H-bonding network, adding another energy term
696 favouring the left side of reaction (2). Concerning Ca^{2+} ions, their observed behaviour is striking
697 as it is very contrasted with the temperature, revealing both the specificity of atmospheric
698 alteration phenomena and the temperature-induced change in their mechanisms. At 80°C, the
699 Ca^{2+} ions remain in the alteration layer and locally form C-S-H-type structures evidenced by the
700 665 cm^{-1} sharp band in the Raman spectra. At 40°C on the contrary, Ca^{2+} ions are totally leached
701 out of the alteration layer, forming calcium carbonates on the surface. This behaviour is in
702 contrast to the one expected considering the calcite solubility, which decreases when temperature
703 rises. The hydration energy of Ca^{2+} is three times that of Na^+ so that Ca^{2+} are markedly stabilized
704 by hydration [70]. Following the preceding discussion, this probably explains that Ca^{2+} ions are
705 more quantitatively extracted out of the hydrated layer than Na^+ at 40°C. Because the enthalpies
706 of hydration and complexation are likely both modest, the dominance of the hydration term is
707 expected to be similar at 40°C and at 80°C. So, why aren't Ca^{2+} ions (and Na^+ ions) also
708 extracted at 80°C? To answer this question, we consider the specificity of atmospheric alteration
709 that lies in the scarcity of water with respect to the silicate solid phase. In the first stage of the
710 alteration, it may be assumed that all the water molecules are bound to the surface or within the
711 hydrated layer, consequently losing part of their solvating properties. Such an effect has been
712 observed in several molecular dynamics simulations of water confined in silica nanopores [71–
713 73]. Then, the complete solvation of the M^+ ion and its detachment from the NBO may be
714 considerably slowed down. If water molecules are engaged in another reaction as the Si-O-Si
715 bond hydrolysis, as proposed below, then the M^+ ions may never be completely solvated and
716 extracted.
717 Next to the acid-base reaction on the NBO sites (reaction (1)), there is another reaction called
718 hydrolysis of the Si-O-Si bonds:
719 $\text{Si-O-Si} + H_2O \leftrightarrow 2\ \text{Si-OH}$ (4)

This reaction *only* is responsible for the silicate network depolymerisation when shifted to the right. It is well-known that this reaction can be catalysed either by protonic assistance (acid pH) or by nucleophilic attack by OH^- ions (basic pH). The activation energy of this reaction is high (86 $kJ.mol^{-1}$ according to [34]) and certainly higher than the activation energy for hydration. Therefore, this reaction is considerably enhanced with temperature, going much faster to the right at 80°C with respect to 40°C. This provides the basis of our hypothesis to explain the different phenomena observed for atmospheric alteration of glass A at 80°C and at 40°C. Indeed, in addition to the different behaviour of Na^+ and Ca^{2+} cations described above, there is a considerable temperature-induced increase of the kinetics of the glass hydration, as measured by the growth of the hydrated, depolymerized layer. We propose that it is due to the increase of the rate of the hydrolysis reaction (4), relatively to the rate of reaction (1). Water molecules are primarily engaged in network hydrolysis rather than in acid-base dissociation onto NBO sites at 80°C. On the contrary at 40°C, the rates of the two reactions converge and water molecules have the time to solvate M^+ and OH^- ions that then migrate towards the surface to form carbonates. Note that Si-O-Si hydrolysis, instead of acid-base dissociation has been inferred from the study of the hydration process of sodium disilicate, forming Q^2 [$(SiO)_2Si$-$(OH)O^-Na^+$] rather than Q^3 [$(SiO)_3Si$-OH] groups. The authors suggested a possible stabilization of these Q^2 groups by the strong H-bonding [63].

Another striking feature of the atmospheric alteration of glass A is the acceleration of the kinetics, observed both at 80°C and at 40°C. The simple "diffusion control" or "surface control" models cannot account for this complex kinetics. Given our understanding of the alteration phenomena described above, the network hydrolysis (reaction (4)) is the rate-controlling step at least at 80°C. This reaction is accelerating with the ageing time and hydrated layer thickness (in the timescale of our experiments). Wang et al. have highlighted the existence of self-accelerating mechanisms in the aqueous alteration of silicate glasses, due to the catalytic effect of OH^- ions that are released by the acid-base reaction step [74,75]. We propose that this effect also operates in atmospheric conditions. After a time period depending on the availability and solvation properties of water in the hydrated layer, M^+ and OH^- ions end up being released and catalyse the network hydrolysis, accelerating the glass hydration rate. It is probable that OH^- ions stay trapped in the H bonding network, as well as their precursor form NBO+H_2O, and that both species contribute to the acceleration of the Si-O-Si bond hydrolysis.

At last, we have attempted to rationalize our observations of the atmospheric alteration phenomenology of glass A using a molecular-scale approach based on the relative rates of reactions (1) and (4). This also corresponds to the basis of the incongruent dissolution model for

754 glasses [76]. Two considerations have been added: the important role of the hydration of cations,
755 and the bound or *ice-like* character of water molecules due to their confinement and scarcity.
756 These considerations are very recent in the glass alteration community. On the other hand, an
757 alternative model for glass dissolution has been proposed on the basis of the very sharp interface
758 between the gel and the pristine glass. It consists in the coupling of surface congruent dissolution
759 and precipitation at the interface (CIDP for Coupled Interface Dissolution Precipitation) [32].
760 We also observe many features that evoke CIDP, as the sharpness of the interface evidenced by
761 the flaking phenomenon and the chemical homogeneity of the hydrated layer. However, we think
762 that the molecular aspects that we have discussed, because they occur at the molecular scale near
763 the alteration front, are relevant to both models. It is possible that the properties of confined
764 water specific to atmospheric conditions preclude any meaningful distinction between the two
765 descriptions of glass alteration.
766
767 **5. CONCLUSION**
768 In this study, the atmospheric alteration (RH = 85 %) of a mixed alkali lime silicate glass
769 representative of a family of unstable compositions of the Cultural Heritage has been described
770 in detail as a function of temperature and time. It is the first time that compositional information
771 on the hydrated layer is accompanied by structural data (multinuclear NMR and Raman
772 spectroscopies) obtained on bulk altered glass powders. First, this study provides a clear evidence
773 that in atmospheric conditions, the hydrolysis of the silicate network (Si-O-Si bonds) is mainly
774 responsible for the glass hydration and controls its kinetics. The leaching of alkali and alkaline-
775 earth cations is limited, probably because of the scarcity and tightly H-bonded character of water,
776 which diminish its solvation property. At 40°C, the cations are leached in the order Ca^{2+} > Na^{+}
777 >> K^{+}, possibly revealing the role of the hydration energy in the leaching process. At 80°C, no
778 leaching is even observed and the hydration by network hydrolysis occurs very rapidly. The
779 thermally activated character of hydrolysis induces an acceleration of this process with respect to
780 other processes (acid-base dissociation of water on NBO sites, cation solvation, cation migration
781 towards the surface). In addition, we suggest that the time acceleration of the hydration kinetics
782 at both temperatures points out another effect: the self-accelerating property of the system
783 towards hydrolysis, due to the catalytic effect of the OH^{-} ions trapped in the H-bonding network,
784 or of their precursor H_2O species that are H-bonded to NBOs. This effect may contribute to the
785 very strong temperature dependency of the hydration kinetics, because at 80°C more NBOs and
786 alkalis are retained in the layer. As a consequence of the partial alkali retention and network
787 depolymerization, the hydrated layer structure is closer to an unstable alkali silicate hydrate than

to an alteration gel (as produced in immersion conditions), at least in the first stages of the alteration. This knowledge is important in the research for efficient surface chemical treatments aimed at preventing glass objects from atmospheric degradation in museum collections.

DATA AVAILABILITY

The raw data required to reproduce these findings are available to download from Mendeley Dataset http://dx.doi.org/10.17632/mnjkhzr6sx.3.

REFERENCES

[1] T. Lombardo, L. Gentaz, A. Verney-Carron, A. Chabas, C. Loisel, D. Neff, E. Leroy, Characterisation of complex alteration layers in medieval glasses, Corros. Sci. 72 (2013) 10–19. doi:10.1016/j.corsci.2013.02.004.

[2] M. Melcher, M. Schreiner, Leaching studies on naturally weathered potash-lime–silica glasses, J. Non. Cryst. Solids. 352 (2006) 368–379. doi:10.1016/j.jnoncrysol.2006.01.017.

[3] P. Bellendorf, H. Roemich, S. Gerlach, P. Mottner, E. López, K. Wittstadt, Archaeological glass: the surface and beyond, Glas. Ceram. Conserv. 2010 Interim Meet. ICOM-CC Work. Group, Oct. 3-6 2010 Corning, New York, U.S.A. (2010) 137–144.

[4] J.J. Kunicki-Goldfinger, Unstable historic glass : symptoms, causes, mechanisms and conservation, Rev. Conserv. 9 (2008) 47–60.

[5] S.P. Koob, Conservation and care of glass objects, Archetype, New-York, 2006.

[6] M. Melcher, M. Schreiner, Glass degradation by liquids and atmospheric agents, in: J.K.H. A. (Ed.), Mod. Methods Fo Anal. Archeol. Hist. Glas., Wiley, 2013: pp. 608–651.

[7] R.H. Brill, The morphology of weathering on historical glasses, Riv. Della Stn. Sper. Del Vetro Sper. Del Vetro. 6 (2000) 7–8.

[8] L. Robinet, The role of organic pollutants in the alteration of historic soda silicate glasses, Edinburgh - Paris VI, 2006.

[9] R.M. Organ, The safe storage of unstable glass, Museums J. 56 (1957) 255–272.

[10] R.H. Brill, Crizzling - A Problem in Glass Conservation, in: Conserv. Archeol. Appl. Arts, Stock. Congr. 2-6 June 1975, International Institute for Conservation, London, 1975: pp. 121–124.

[11] S.P. Koob, Crizzling glasses : problems and solutions, Eur. J. Glas. Sci. Technol. A. 53 (2012) 225–227.

[12] V. Oakley, Fighting the inevitable : the continuing search for a solution to glass decay at the V&A, Glas. Technol. 42 (2001) 65–69.

http://cat.inist.fr/?aModele=afficheN&cpsidt=14078296 (accessed November 16, 2014).

[13] S. Davison, R.G. Newton, Conservation and restauration of glass, Butterwort, 2003.

[14] M. Verità, R. Falcone, G. Sommariva, M.H. Chopinet, P. Lehuédé, Weathering of the inner surface of soda-lime-silica glass containers exposed to the atmosphere, Glas. Technol. Eur. J. Glas. Sci. Technol. Part A. 50 (2009) 65–70.

[15] M.-H. Chopinet, P. Lehuédé, Les problèmes d'altération rencontrés sur des verres industriels, Verre. 16 (2010) 20–27.

[16] M.-H. Chopinet, M. Verità, R. Falcone, P. Lehuédé, M. Vallotto, M. Nardone, A. Sodo, Soda-lime-silica glass containers: chemical durability and weathering products, Adv. Mater. Res. 39–40 (2008) 305–310. doi:10.4028/www.scientific.net/AMR.39-40.305.

[17] C. Wang, G. Krausch, E. Rädlein, S. Tratzky, M. Schramm, A. Weber, Study of surface changes on industrial glasses with AFM, FE-SEM, EDX, SNMS and LM, Glas. Sci. Technol. 6 (2004) 273–282.

[18] A.A. Chaou, A. Abdelouas, Y. El Mendili, R. Bouakkaz, S. Utsunomiya, C. Martin, X. Bourbon, Vapor hydration of a simulated borosilicate nuclear waste glass in unsaturated conditions at 50°C and 90°C, RSC Adv. 5 (2015) 64538–64549.

[19] T.A. Abrajano, J.K. Bates, J.J. Mazer, Aqueous corrosion of natural and nuclear waste glasses II. Mechanisms of vapor hydration of nuclear waste glasses, J. Non. Cryst. Solids. 108 (1989) 269–288. doi:10.1016/0022-3093(89)90297-4.

[20] R. Bouakkaz, A. Abdelouas, A.A. Chaou, Y. El Mendili, A borosilicate glass hydration at low temperature, J. Chem. Pharm. Res. 7 (2015) 332–337.

[21] M. Verità, Modern and ancient glass: nature, compostion and deterioration mechanisms, in: R.-A. Lefèvre (Ed.), Mater. Cult. Herit. Their Environ., Edipuglia, Bari, 2006: pp. 119–132.

[22] R. Falcone, F. Licenziati, E.F. Orsega, M. Verità, The dependence of the weathering of soda-lime-silica glass on environmental parameters: A preliminary investigation, Eur. J. Glas. Sci. Technol. Part A. 52 (2011) 23–29.

[23] L. Robinet, C. Hall, K. Eremin, S. Fearn, J. Tate, Alteration of soda silicate glasses by organic pollutants in museums: Mechanisms and kinetics, J. Non. Cryst. Solids. 355 (2009) 1479–1488. doi:10.1016/j.jnoncrysol.2009.05.011.

[24] S. Fearn, D.S. McPhail, B. Hagenhoff, E. Tallarek, TOF-SIMS analysis of corroding museum glass, Appl. Surf. Sci. 252 (2006) 7136–7139. doi:10.1016/j.apsusc.2006.02.157.

[25] A. Rodrigues, S. Fearn, M. Vilarigues, Historic K-rich silicate glass surface alteration: Behaviour of high-silica content matrices, Corros. Sci. 145 (2018) 249–261.

doi:10.1016/j.corsci.2018.10.010.
[26] A. Rodrigues, S. Fearn, T. Palomar, M. Vilarigues, Early stages of surface alteration of soda-rich-silicate glasses in the museum environment, Corros. Sci. 143 (2018) 362–375. doi:10.1016/j.corsci.2018.08.012.
[27] I. Biron, Émaux sur Métal – du IXe au XIXe Siècle. Histoire, Technique et Matériaux, Faton, 2015.
[28] F. Alloteau, P. Lehuédé, O. Majérus, T. Charpentier, D. Caurant, I. Biron, New insight into atmospheric alteration of alkali-lime silicate glasses, Corros. Sci. 122 (2017) 12–25. doi:10.1016/j.corsci.2017.03.025.
[29] L. Greenspan, Humidity fixed points of binary saturated aqueous solutions, J. Res. Natl. Bur. Stand. Sect. A Phys. Chem. 81A (1977) 89. doi:10.6028/jres.081A.011.
[30] L.R. Riciputi, J.. M. Elam, L.M. Anovitz, D.R. Cole, Obsidian diffusion dating by secondary ion mass spectrometry: A test using results from Mound 65, Chalco, Mexico, J. Archaeol. Sci. 29 (2002) 1055–1075. doi:10.1006/jasc.2001.0692.
[31] F.M. Ernsberger, Properties of glass surf aces, Annu. Rev. Mater. Sci. 2 (1972) 529–572.
[32] C. Lenting, O. Plümper, M. Kilburn, P. Guagliardo, M. Klinkenberg, Towards a unifying mechanistic model for silicate glass corrosion, Npj Mater. Degrad. 28 (2018). doi:10.1038/s41529-018-0048-z.
[33] H. Scholze, Chemical durability of glasses, J. Non. Cryst. Solids. 52 (1982) 91–103.
[34] A. Verney-Carron, S. Gin, P. Frugier, G. Libourel, Long-term modeling of alteration-transport coupling: Application to a fractured Roman glass, Geochim. Cosmochim. Acta. 74 (2010) 2291–2315. doi:10.1016/j.gca.2010.01.001.
[35] X. Xue, M. Kanzaki, Proton distributions and hydrogen bonding in crystalline and glassy hydrous silicates and related inorganic materials: Insights from high-resolution solid-state nuclear magnetic resonance spectroscopy, J. Am. Ceram. Soc. 92 (2009) 2803–2830. doi:10.1111/j.1551-2916.2009.03468.x.
[36] T. Schaller, A. Sebald, One- and two-dimensional 1H magic-angle spinning experiments on hydrous silicate glasses, Solid State Nucl. Magn. Reson. 5 (1995) 89–102. doi:10.1016/0926-2040(95)00028-O.
[37] H. Eckert, J.P. Yesinowski, L.A. Silver, E.M. Stolper, Water in silicate glasses: quantitation and structural studies by proton solid echo and magic angle spinning NMR methods, J. Phys. Chem. 92 (1988) 2055–2064. doi:10.1021/j100318a070.
[38] X. Ai, F. Deng, J. Dong, W. Hu, H. Xu, C. Ye, One- and two-dimensional solid-state magic angle spinning NMR studies on the hydration process of layered sodium disilicate

SKS-6., Solid State Nucl. Magn. Reson. 25 (2004) 216–26. doi:10.1016/j.ssnmr.2003.10.002.

[39] G.G. Almond, R.K. Harris, K.R. Franklin, A structural consideration of kanemite, octosilicate, magadiite and kenyaite, J. Mater. Chem. 7 (1997) 681–687. doi:10.1039/a606856a.

[40] X. Xue, M. Kanzaki, Dissolution mechanisms of water in depolymerized silicate melts: Constraints from1H and29Si NMR spectroscopy and ab initio calculations, Geochim. Cosmochim. Acta. 68 (2004) 5027–5057. doi:10.1016/j.gca.2004.08.016.

[41] C. Le Losq, G.D. Cody, B.O. Mysen, Alkali influence on the water speciation and the environment of protons in silicate glasses revealed by 1H MAS NMR spectroscopy, Am. Mineral. 100 (2015) 466–473. doi:10.2138/am-2015-5004.

[42] E. Robert, A. Whittington, F. Fayon, M. Pichavant, D. Massiot, Structural characterization of water-bearing silicate and aluminosilicate glasses by high-resolution solid-state NMR, Chem. Geol. 174 (2001) 291–305. doi:10.1016/S0009-2541(00)00321-1.

[43] S.C. Kohn, R. Dupree, M.E. Smith, Proton environments and hydrogen-bonding in hydrous silicate glasses from proton NMR, Nature. 337 (1989) 539–541. doi:10.1038/337539a0.

[44] F. Angeli, M. Gaillard, P. Jollivet, T. Charpentier, Influence of glass composition and alteration solution on leached silicate glass structure: A solid-state NMR investigation, Geochim. Cosmochim. Acta. 70 (2006) 2577–2590. doi:10.1016/j.gca.2006.02.023.

[45] C. Gardiennet, P. Tekely, Structural and Motional Features of a Layered Sodium Hydrous Silicate as Revealed by Solid State NMR, J. Phys. Chem. B. 106 (2002) 8928–8936.

[46] H. Maekawa, T. Maekawa, K. Kawamura, T. Yokokawa, The structural groups of alkali silicate glasses determined from 29Si NMR, J. Non. Cryst. Solids. 127 (1991) 53–64.

[47] D.R. Spearing, I. Farnan, J.F. Stebbins, Dynamics of the α-β phase transitions in quartz and cristobalite as observed by in-situ high temperature 29Si and 17O NMR, Phys. Chem. Miner. 19 (1992) 307–321. doi:10.1007/BF00204008.

[48] F. Angeli, O. Villain, S. Schuller, S. Ispas, T. Charpentier, Insight into sodium silicate glass structural organization by multinuclear NMR combined with first-principles calculations, Geochim. Cosmochim. Acta. 75 (2011) 2453–2469. doi:10.1016/j.gca.2011.02.003.

[49] F. Angeli, J.M. Delaye, T. Charpentier, J.-C. Petit, D. Ghaleb, P. Faucon, Influence of glass chemical composition on the Na-O bond distance: a 23Na 3Q-MAS NMR and molecular dynamics study, J. Non. Cryst. Solids. 276 (2000) 132–144. doi:10.1097/00001756-200112210-00023.

[50] F. Angeli, M. Gaillard, P. Jollivet, T. Charpentier, Ca MAS NMR for probing the structural configuration of calcium in glass, Chem. Phys. Lett. 440 (2007) 324–328. doi:10.1016/j.cplett.2007.04.036.

[51] T. Furukawa, K.E. Fox, W.B. White, Raman spectroscopic investigation of the structure of silicate glasses. III. Raman intensities and structural units in sodium silicate glasses, J. Chem. Phys. 75 (1981) 3226–3237. doi:10.1063/1.442472.

[52] P. Mcmillan, Structural studies of silicate glasses and melts-applications and limitations of Raman spectroscopy, Am. Mineral. 69 (1984) 622–644.

[53] L. Robinet, C. Coupry, K. Eremin, C. Hall, The use of Raman spectrometry to predict the stability of historic glasses, J. Raman Spectrosc. 37 (2006) 789–797. doi:10.1002/jrs.1540.

[54] B. Hehlen, D.R. Neuville, D. Kilymis, S. Ispas, Bimodal distribution of Si–O–Si angles in sodo-silicate glasses, J. Non. Cryst. Solids. 469 (2017) 39–44. doi:10.1016/j.jnoncrysol.2017.04.009.

[55] N. Zotov, H. Keppler, The influence of water on the structure of hydrous sodium tetrasilicate glasses, Am. Miner. 83 (1998) 823–834. doi:scopus/2-s2.0-0031797062.

[56] C. Le Losq, D.R. Neuville, Effect of the Na/K mixing on the structure and the rheology of tectosilicate silica-rich melts, Chem. Geol. 346 (2013) 57–71. doi:10.1016/j.chemgeo.2012.09.009.

[57] G. Spiekermann, M. Steele-Macinnis, C. Schmidt, S. Jahn, Vibrational mode frequencies of silica species in SiO 2-H 2O liquids and glasses from ab initio molecular dynamics, J. Chem. Phys. 136 (2012). doi:10.1063/1.3703667.

[58] C. Le Losq, B.O. Mysen, G.D. Cody, Water and magmas: insights about the water solution mechanisms in alkali silicate melts from infrared, Raman, and29Si solid-state NMR spectroscopies, Prog. Earth Planet. Sci. 2 (2015). doi:10.1186/s40645-015-0052-7.

[59] L. Robinet, K. Eremin, C. Coupry, C. Hall, N. Lacome, Effect of organic acid vapors on the alteration of soda silicate glass, J. Non. Cryst. Solids. 353 (2007) 1546–1559. doi:10.1016/j.jnoncrysol.2007.01.039.

[60] H. Ohashi, M. Sekita, Raman Spectroscopic Study of the Si-O-Si Stretching Vibration in Clinopyroxenes, J. Japan Assoc. Mineral. Petrol. Sci. 77 (1982) 455–459.

[61] C. Breen, K. Garbev, J. Yarwood, B. Gasharova, P. Stemmermann, L. Black, Structural Features of C?S?H(I) and Its Carbonation in Air?A Raman Spectroscopic Study. Part I: Fresh Phases, J. Am. Ceram. Soc. 90 (2007) 900–907. doi:10.1111/j.1551-2916.2006.01428.x.

[62] F. Angéli, M. Gaillard, P. Jollivet, T. Charpentier, Influence of glass composition and

alteration solution on leached silicate glass structure: A solid-state NMR investigation, Geochim. Cosmochim. Acta. 70 (2006) 2577–2590. doi:10.1016/j.gca.2006.02.023.

[63] X. Ai, F. Deng, J. Dong, L. Chen, C. Ye, Stability of layered sodium disilicate during hydration process as studied by multinuclear solid state NMR spectroscopy, J. Phys. Chem. B. 106 (2002) 9237–9244. doi:10.1021/jp020458i.

[64] B.C. Bunker, Molecular mechanisms for corrosion of silica and silicate glasses, J. Non. Cryst. Solids. 179 (1994) 300–308. doi:10.1016/0022-3093(94)90708-0.

[65] B.M.J. Smets, T.P.A. Lommen, The role of molecular water in the leaching of glass, Phys. Chem. Glas. 24 (1983) 35–36.

[66] B.M.J. Smets, On the mechanism of the corrosion of glass by water, Philips Tech. Rev. 42 (1985) 59–64.

[67] B.J. Teppen, D.M. Miller, Hydration Energy Determines Isovalent Cation Exchange Selectivity by Clay Minerals, Soil Sci. Soc. Am. J. 70 (2006) 31–40.

[68] B. Rotenberg, J.P. Morel, V. Marry, P. Turq, N. Morel-Desrosiers, On the driving force of cation exchange in clays: Insights from combined microcalorimetry experiments and molecular simulation, Geochim. Cosmochim. Acta. 73 (2009) 4034–4044. doi:10.1016/j.gca.2009.04.012.

[69] M. Collin, M. Fournier, T. Charpentier, M. Moskura, S. Gin, Impact of alkali on the passivation of silicate glass, Npj Mater. Degrad. 2 (2018) 16. doi:10.1038/s41529-018-0036-3.

[70] Y. Marcus, Thermodynamics of Solvation of Ions. Part 5. Gibbs free energy of hydration at 298.15 K, J. Chem. Soc. Faraday Trans. 87 (1991) 2995–2999. doi:10.1524/zpch.1992.176.part_1.130.

[71] M. Collin, S. Gin, B. Dazas, T. Mahadevan, J. Du, I.C. Bourg, Molecular Dynamics Simulations of Water Structure and Diffusion in a 1 nm Diameter Silica Nanopore as a Function of Surface Charge and Alkali Metal Counterion Identity, J. Phys. Chem. C. 122 (2018) 17764–17776. doi:10.1021/acs.jpcc.8b03902.

[72] I.C. Bourg, C.I. Steefel, Molecular dynamics simulations of water structure and diffusion in silica nanopores, J. Phys. Chem. C. 116 (2012) 11556–11564. doi:10.1021/jp301299a.

[73] S. Senapati, A. Chandra, Dielectric constant of water confined in a nanocavity, J. Phys. Chem. B. 105 (2001) 5106–5109. doi:10.1021/jp011058i.

[74] Y. Wang, C.F. Jove-Colon, C. Lenting, J. Icenhower, K.L. Kuhlman, Morphological instability of aqueous dissolution of silicate glasses and minerals, Npj Mater. Degrad. 2 (2018) 27. doi:10.1038/s41529-018-0047-0.

[75] Y. Wang, C.F. Jove-Colon, K.L. Kuhlman, Nonlinear dynamics and instability of aqueous dissolution of silicate glasses and minerals, Sci. Rep. 6 (2015) 30256. doi:10.1038/s41529-018-0047-0.

[76] S. Gin, L. Neill, M. Fournier, P. Frugier, T. Ducasse, M. Tribet, A. Abdelouas, B. Parruzot, J. Neeway, N. Wall, The controversial role of inter-diffusion in glass alteration, Chem. Geol. 440 (2016) 115–123. doi:10.1016/j.chemgeo.2016.07.014.

ACKNOWLEDGEMENTS

The authors gratefully thank PSL University for the funding of this work, Marie-Hélène Chopinet, Sophie Papin and Kamila Plevacova (Saint-Gobain Recherche, France) for the glass fabrication. Mélanie Moskura (NIMBE, CEA) is acknowledged for her help in conducting the NMR experiments.

SUPPLEMENTARY MATERIALS

See Data in Brief zip file.